



Evaluation of Reaction Parameters Dependent Optical Properties and Its Photovoltaics Performances of CdTe QDs

Ayyaswamy Arivarasan¹ · Sambandam Bharathi² · V. Vijayaraj³ · Ganapathy Sasikala³ · Ramasamy Jayavel⁴

Received: 17 November 2017 / Accepted: 4 February 2018 / Published online: 19 February 2018
© Springer Science+Business Media, LLC, part of Springer Nature 2018

Abstract

High quality thiol capped cadmium telluride quantum dots were prepared in aqueous phase by the optimization of reaction parameters and their photovoltaics performances were studied through the fabrication of quantum dots sensitized solar cells. Mercaptosuccinic acid capped cadmium telluride quantum dots were prepared under different reaction conditions (at acidic and basic solutions, different precursors ratios, under different reaction temperatures and are various refluxing times) and their optical absorption and emission properties were studied. Based on these observations, the reaction parameters were optimized and high quality mercaptosuccinic acid capped cadmium telluride quantum dots were prepared at the optimized reaction conditions. Crystalline structure of the prepared cadmium telluride quantum dots was studied by X-ray diffraction analysis, which confirms the cubic zinc blende structure. Size dependent optical properties of mercaptosuccinic acid capped cadmium telluride quantum dots were revealed by UV–Vis absorption and fluorescence emission studies. The formation of cadmium telluride quantum dots with the thiol capping layer over the quantum dots was studied by the X-ray photoelectron spectroscopy and Fourier Transform Infra Red spectroscopy analysis. Cadmium telluride quantum dots sensitized solar cells were fabricated by using polysulfide electrolytes with TiO₂ as the photoanode. The photovoltaic performance of cadmium telluride quantum dots sensitized photoelectrodes was studied by the J–V characteristic curves under the illumination of light with 1 Sun intensity. Mercaptosuccinic acid capped cadmium telluride quantum dots prepared at optimized reaction conditions showed an enhanced solar cell efficiency of 0.87% at 3 h of absorption time.

Keywords Quantum dots · Cadmium telluride · Reaction parameters · Quantum dots sensitized solar cells

1 Introduction

Quantum dots (QDs) are zero dimensional semiconducting nanostructures, which are extensively studied for their size and shape dependent optical behaviors. These special characteristics of the QDs attract a large attention for numerous applications including photovoltaics, LEDs, biological imaging, chemical and biosensors, etc.,

[1–4]. In particular, they are very attractive in optoelectronic devices due to their high fluorescent nature. Generally II–VI semiconductors are the special choice of the researchers for the optoelectronic applications, because their absorption and emission spectra can be tuned in visible and NIR regions depends on the size and composition of the materials. Particularly cadmium chalcogenide based QDs (CdS, CdSe and CdTe) attracts a huge interest in scientific community due to its highly fluorescent nature. Even though, cadmium sulfide (CdS) [5–7] and cadmium selenide QDs (CdSe) [8–10] are widely used in energy applications, Cadmium Telluride (CdTe) QDs play a vital role in industrial applications due to their large exciton Bohr radius (7.3 nm) and narrow bulk band gap of 1.475 eV. Also, CdTe QDs was used as the potential sensitizers in third generation solar cells [11]. Up to date various attempts are made to produce highly fluorescent CdTe QDs and these attempts are majorly classified into two categories such as organometallic route based on the

✉ Ayyaswamy Arivarasan
arivarasan.nanotech@gmail.com

¹ Department of Physics, International Research Center, Kalasalingam University, Krishnankoil, Tamilnadu, India

² Department of Physics and Nanotechnology, SRM University, Chennai, Tamilnadu, India

³ Crystal Growth Centre, Anna University, Chennai 600025, India

⁴ Centre for Nanoscience and Technology, Anna University, Chennai 600025, India

high-temperature thermolysis of precursors [12, 13] or on a dehalosilylation reaction [14] and the synthesis in an aqueous medium using polyphosphates [15] or thiols [16–18] as stabilizing agents. The CdTe QDs prepared in aqueous phase possess higher stability, water solubility and biocompatibility etc.

In aqueous synthesis route, the reaction parameters such as the precursor concentrations, pH, reaction temperature etc play a vital role on the size and stability of the prepared QDs. Obviously; they are influencing the optical behavior of the prepared QDs. Because, the optical behavior of the QDs is surface dependent one. So the optical behavior of the prepared QDs can be tuned by the optimization of the reaction parameters. In order to produce a high quality CdTe QD, it is necessary to optimize the reaction parameters.

Most of the recent reports deals with the preparation of CdTe QDs, utilize the air sensitive sodium hydrogen telluride (NaHTe) or metal Te, as the tellurium source. Generally, it is an unstable compound under ambient conditions [19, 20], and this hurdle was eliminated by the creation of inert atmosphere during the reaction procedures.

In this work, Mercapto Succinic Acid (MSA) capped CdTe QDs was prepared in aqueous phase by using air stable potassium tellurite as the precursor material and the synthesis procedures were carried out in the ambient atmosphere, instead of inert atmosphere. The reaction parameters such as, the precursor concentration, reaction pH and the reaction temperatures are optimized and their optical responses were studied. The quality of the prepared CdTe QDs were studied and confirmed by various analytical characterization techniques including, X-ray diffraction Analysis (XRD), UV–Vis absorption spectroscopy, fluorescence emission, Fourier Transform Infra-Red (FTIR) spectroscopy, X-ray photoelectron Spectroscopy (XPS), High Resolution Transmission Electron Microscopy (HRTEM), etc. The solar cell efficiency of the prepared CdTe QDs was studied by the fabrication of quantum dots sensitized solar cells by using TiO₂ as the wide band gap semiconductor.

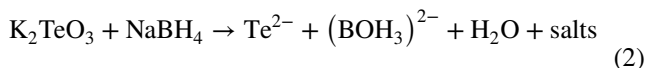
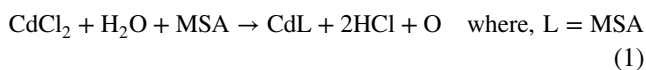
2 Materials and Methods

2.1 Precursor Materials

Cadmium chloride monohydrate (CdCl₂·H₂O), tri sodium citrate and sodium borohydride (NaBH₄) were purchased from Merck specialities private limited, India. Commercially available potassium tellurite (K₂TeO₃) and mercaptosuccinic acid (MSA) were procured from Alfa Aesar chemicals. The other analytical grade chemicals were purchased from CDH chemicals, India and Millipore water with resistivity of 18 MΩ cm was used as a solvent for the synthesis.

2.2 Synthesis of MSA Capped CdTe QDs

All experiments were carried out in an aqueous medium at ambient pressure. CdTe QDs was prepared by the reaction between Cd²⁺ ions and Te²⁻ ions using MSA as a capping agent [21, 22]. The effect of precursor concentration on the optical properties of CdTe QDs was studied in a controlled atmosphere. The reaction mechanism of MSA capped CdTe QDs is given below



In a detailed description, aqueous Cd²⁺ solution was prepared by dissolving CdCl₂ salt in 100 ml of Millipore water. To reduce the formation of cadmium thiolate complexes during the reaction, 0.1 g of tri-sodium citrate was added in the aqueous CdCl₂ solution. The appropriate amount of the MSA was added in the reaction mixture under constant stirring to prepare the MSA capped Cd complexes. The pH of the solution was altered by using 2 M NaOH solution. At the desired pH, potassium salts of tellurium were added as the Te source to the reaction mixture. Along with the Te source, 0.1 g of NaBH₄ was added to reduce Te salts into Te²⁻ ions. At this stage, the transparent reaction mixture transformed into light green in color, indicating the formation of CdTe monomers.

The monomer solution of CdTe QDs was transformed into a three neck round bottom flask and refluxed at constant temperature. During the refluxing, a condenser was attached to the round bottom flask to reduce the solvent evaporation. Depending on the refluxing time, the color of the reaction mixture was changed to intermediate between light green and dark red in the visible range, which indicates that the size of the CdTe QDs was increased during the refluxing. Samples were collected at regular intervals during the refluxing for optical studies. Resultant solution was precipitated using acetone. The precipitation process was repeated several times with water to remove the un-reactant materials. The precipitate was collected and dried at room temperature. The influence of reaction parameters such as precursor concentration, capping agent concentration, reaction pH and the reaction temperature on the optical properties of CdTe QDs was systematically investigated.

2.3 Synthesis of TiO₂ Nanoparticles

Wet chemical synthesis technique was adopted for the preparation of Titanium dioxide (TiO₂) nanoparticles. In a typical synthesis 10 ml of titanium (IV) butoxide was dissolved in 50 ml of absolute ethanol. The reaction mixture was ultrasonically agitated for 10 min. Then 5 ml of freshly prepared NaOH solution was added drop-wise into the reaction mixture under constant stirring. During the process, the reaction pH was maintained at 7. All these reactions were carried out at room temperature under ambient conditions. The resultant solution was filtered and the precipitates were collected and washed with ethanol and de-ionized water. The washing process was repeated for several times to remove the un-reactant materials. The final product was dried at 100 °C for 12 h and stored for further process.

2.4 Fabrication of Quantum Dots Sensitized Solar Cells

In order to estimate the photovoltaic performance of MSA capped CdTe colloidal QDs, sandwich type solar cells were fabricated with two electrodes such as working electrode and counter electrodes [23]. QDs sensitized TiO₂ layer on the indium tin oxide (ITO) coated glass substrate was used as the working electrode and the graphite coated ITO was used as the counter electrode.

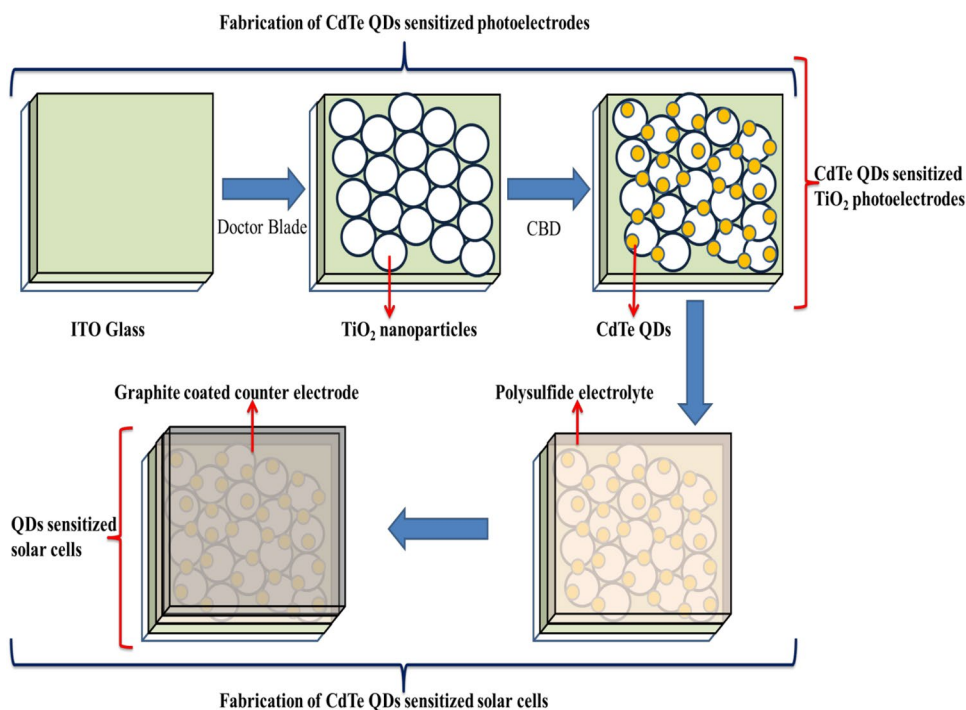
2.4.1 Preparation of Working Electrode

Glass substrate with indium tin oxide coating was used as the conducting electrodes for the fabrication of QDSSCs. The sheet resistance of the ITO substrate was 15 Ω/m². The ITO substrate was properly cleaned by sonication using ethanol and water. In this work nanocrystalline TiO₂ was used as the wide band gap semiconductor layer to fabricate the photoelectrodes. Nanocrystalline TiO₂ was deposited onto the ITO substrate by the doctor blade technique.

TiO₂ paste was prepared by the fine grinding of TiO₂ nanoparticles in the presence of acetyl acetone and Millipore water [24]. A few drops of soap solution (Triton X 100) were added to improve the affinity. The prepared TiO₂ paste was deposited over the ITO substrate by using a flat glass substrate. Thickness of the TiO₂ layer was controlled by a scotch tape (thickness 50 μm), which is used to cover the corner of the ITO substrates.

To improve the photovoltaic performance, the prepared TiO₂ layer was sintered at 500 °C for 30 min and cooled to room temperature. The sintered nanocrystalline TiO₂ layer was immersed in the bi-functional linker molecular solution (capping agent solution, 1 M MSA) and then sensitized with MSA capped CdTe QDs. For this purpose 1M CdTe solution was prepared in water and the nanocrystalline TiO₂ layer with MSA bi-linker molecules was immersed in the CdTe solution for sensitization. Deposition time was varied to control the sensitization rate of the CdTe QDs. Finally, the QDs sensitized photoelectrodes were rinsed with water and dried at ambient atmosphere. The steps involved in the

Fig. 1 Fabrication procedures for CdTe QDs sensitized solar cells



fabrication of CdTe QDs sensitized solar cells were represented in Fig. 1.

2.4.2 Preparation of Polysulfide Electrolytes

In DSSCs, iodide/triiodide based liquid electrolytes are commonly used as redox mediators. However, the use of iodide based electrolyte does not give good performance in Cd chalcogenide QDSSCs. The efficiency is usually very poor—less than 1%. This is because of the fact that iodide based electrolyte itself is corrosive towards the Cd chalcogenide QDs, especially for CdTe QDSSCs. To remedy this problem, polysulfide electrolytes were used instead of polyiodide electrolytes [25]. The polysulfide electrolyte contains the homogeneous mixture of 1M Na₂S, 1 M sulfur and 0.2 M KCl in a homogeneous solution of methanol and water (7:3, v/v).

2.4.3 Preparation of Counter Electrode

Transparent glasses coated with conductive indium tin oxide (ITO) were used as a substrate for the counter electrodes. These glasses were cleaned by sonication in ethanol and water. The counter electrodes were prepared by deposition of graphite layers by using a lightening candle and cooled to room temperature. The graphite layer thickness were controlled by the deposition time. The indium tin oxide coated glasses with the optimized thickness of graphite layers were used as the counter electrode for the fabrication of quantum dots sensitized solar cells.

2.4.4 Assembling of QDSSCs

QDSSC are fabricated by assembling the CdTe QDs sensitized TiO₂ working electrode and the graphite coated counter electrode together by using a 50 μm thick hot melt tape as the spacer. The assembled electrodes were heated to 100 °C to attach the electrodes and cool down to room temperature. The space between the electrodes was filled with polysulfide electrolytes by the capillary flow technique, and sealed using silicone to avoid the leakage.

2.5 Characterization Techniques

2.5.1 Characterization of MSA Capped CdTe QDs

The crystalline structure was confirmed through powder XRD patterns recorded by the Rigaku Miniflex II-C X-ray diffractometer in the range 20° to 70° at a scanning rate of 3°/min. The absorption spectra of the as-prepared QDs was recorded using UV-WIN T90+ UV-Vis spectrophotometer and their corresponding fluorescence spectra was recorded using Horiba Fluorolog-3 spectrofluorometer under an excitation wavelength of 420 nm. HRTEM images of the

prepared QDs was captured using FEI-TECHNAI G2 electron microscope operating at 250 kV. Perkin Elmer Spectrum1 FT-IR spectrometer was used to record the FT-IR spectra of the prepared QDs in the range of 500–4000 cm⁻¹. Omicron Nanotechnology, GMPH spectrometer with Al K_α monochromatic radiation was used to perform the XPS analysis. The calibration for XPS analysis was done by the carbon C 1s peak at 284.6 eV. Thermal stability of the prepared samples was analysed using a TG-DTA: SII 6300 EXSTAR thermal analyzer under the scanning rate of 10°C/min.

2.5.2 Photovoltaic Characterization

The current–voltage characteristics were performed using a Keithley 2400 source meter under simulated AM 1.5 G illumination (100 mW cm⁻²) provided by a solar simulator (Oriel, Model: 91192). A 1000 W Xenon arc lamp (Oriel, Model: 6271) served as a light source and its incident-light intensity was calibrated with an NREL-calibrated Si solar cell equipped with an optical filter to approximate AM 1.5 G one sun light intensity before each experiment.

3 Results and Discussion

3.1 Effect of Reaction Parameters

The optical behavior of the MSA capped CdTe QDs was affected by the various parameters including precursors ratio, capping agent ratio, reaction pH and reaction temperature. In order to study the effect of precursor ratio, MSA capped CdTe QDs were prepared by using different precursor ratios. In this process, the reaction ratio of Cd²⁺ to Te²⁻ was varied between 0.5:1 and 10:1. According to the experimental results, the fluorescence intensity of the MSA capped CdTe QDs was increased with precursor concentration as shown in Fig. 2a, b. This is due to the saturation limit of the precursors. The highest fluorescence intensity was obtained in the precursor ratio of 2.5:1. Beyond this concentration cadmium rich CdTe QDs was produced, which results in the reduction of fluorescence intensity of the MSA capped CdTe QDs.

The effect of MSA concentration on the optical properties of the CdTe QDs was studied by varying the reaction ratio of Cd²⁺ to MSA between 1:0.04 and 1:2 and the corresponding fluorescence intensity variations are shown in Fig. 2c. At the same time all the other parameters are fixed as a constant. During the synthesis process the surface passivation of cadmium-thiolate complexes over the CdTe QDs was increased with increasing the molar ratio of the MSA, which reduces the surface defects. Obviously, the higher surface passivation increase the fluorescence intensity of the MSA capped CdTe QDs. This could be attained up to a

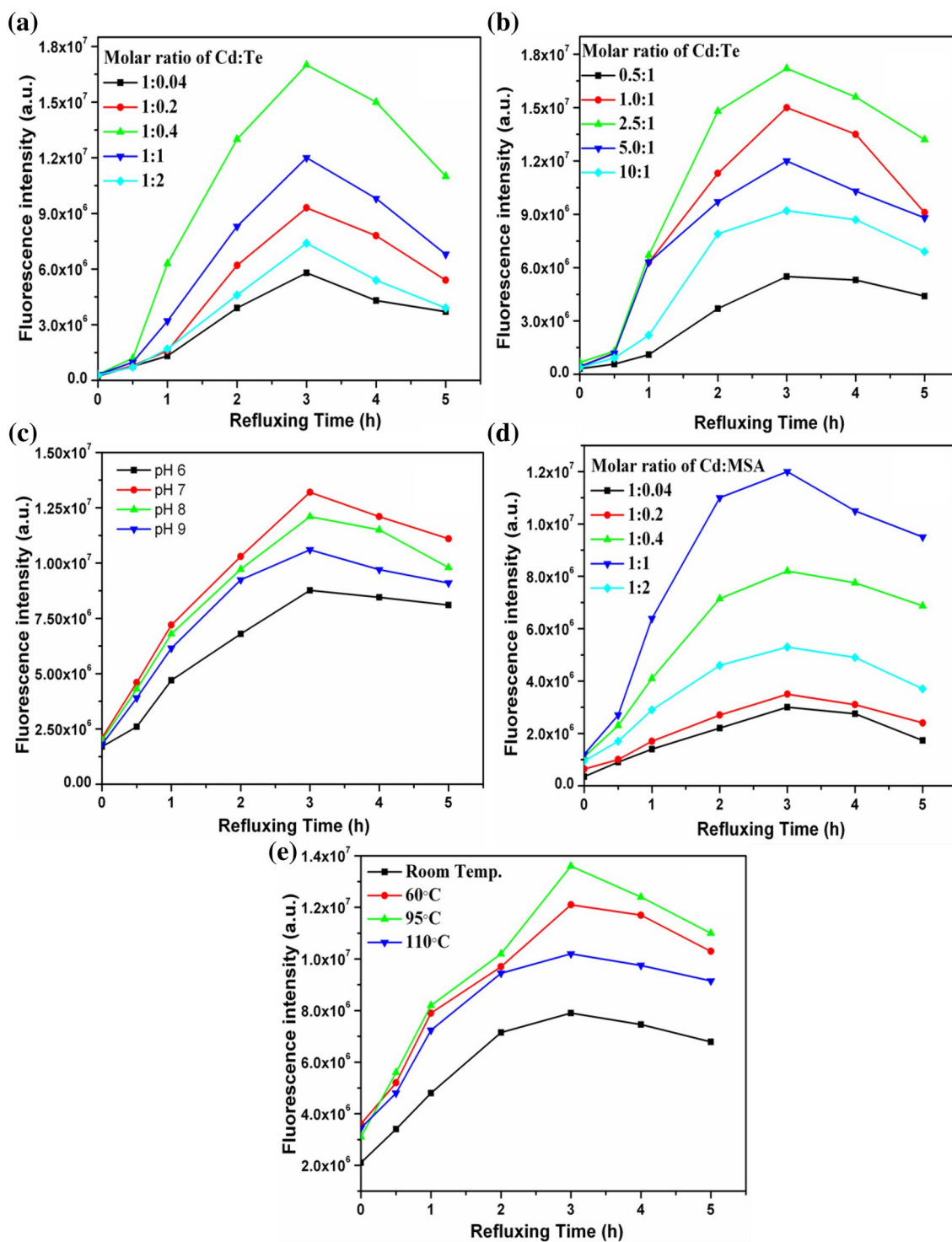


Fig. 2 Effect of different reaction parameters on the fluorescence intensity of the CdTe QDs. **a, b** Effect of precursor ratio, **c** effect of Cd²⁺: MSA ratio, **d** effect of reaction pH and **e** Effect of reaction temperature

certain MSA concentration (1:1). Beyond this concentration, it reduces the reaction rate of MSA capped CdTe QDs.

To study the effect of reaction temperatures on the optical properties of the CdTe QDs, the reactions were carried

out at different temperatures. CdTe QDs synthesized at room temperature showed a weak fluorescence when compared to other reaction temperatures. Consequently the fluorescent intensity was increased with reaction

temperatures. This is due to the presence of a large number of defects at lower temperatures, which leads to the slow growth of CdTe QDs. At the same time the crystallinity was increased at higher temperature results in the enhancement of the quantum yield [26]. On the other hand, at very high temperature, decomposition of thiol stabilizer may occur and resulted in the decrement of the quantum yield [27]. On the optimization of reaction temperature, equilibrium in attachment and detachment rate of cadmium thiolate complexes around the surface of CdTe QDs was obtained. According to the optimization of reaction temperatures, high quality CdTe QDs was obtained at 95 °C as shown in Fig. 2e. As discussed above, high quality MSA capped CdTe QDs were prepared by optimizing the reaction parameters and the optimized reaction conditions are 2.5:1, 1:1, 95 °C and 7 corresponds to the precursor concentration, Cd²⁺ to MSA ratio, reaction pH and the reaction temperature respectively. The highest absorption and emission maximum values with their corresponding bandgap values under different reaction parameters were listed in Table 1.

Table 1 Highest absorption and emission maximum values and their corresponding band gap values of CdTe QDs under different reaction parameters

Parameters	Concentration/ values	λ_{\max} (nm)		E_g (eV)
		Absorption	Emission	
Cd ²⁺	0.005 M	465	505	2.67
	0.01 M	470	515	2.64
	0.025 M	475	522	2.61
	0.05 M	484	528	2.56
	0.10 M	501	536	2.47
Te ²⁻	0.005 M	469	492	2.64
	0.01 M	482	499	2.58
	0.025 M	486	505	2.55
	0.05 M	496	511	2.50
MSA	0.005 M	458	492	2.71
	0.01 M	468	501	2.65
	0.025 M	479	508	2.59
	0.05 M	483	515	2.57
pH	6	406	482	3.05
	7	412	484	3.01
	8	419	485	2.96
	9	425	487	2.92
Temperature	Room Temp.	497	535	2.49
	60 °C	498	540	2.49
	95 °C	499	545	2.48
	110 °C	496	540	2.49

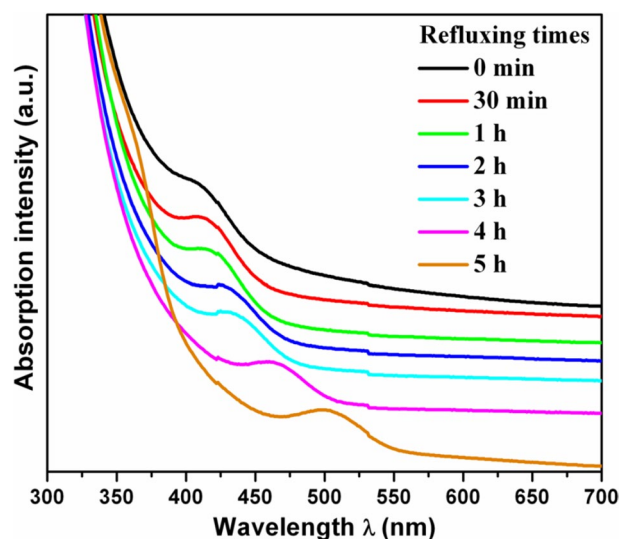


Fig. 3 UV–Vis absorption spectra of MSA capped CdTe QDs for different refluxing time

3.2 UV–Vis Absorption Studies

UV–Vis absorption spectra of MSA capped CdTe colloidal QDs were recorded for different refluxing times as shown in Fig. 3. All samples show a well pronounced absorption maximum. At the starting stage of the refluxing time, the absorption spectrum shows a absorption band edge at around 400 nm. The noticeable red shift was observed in the absorption band edge depending on the increment in refluxing time due to the size variation of QDs. This clearly indicates that the size of MSA capped CdTe colloidal QDs was increased with the refluxing time. At the starting stage of the refluxing time, CdTe monomers were created. Then the CdTe monomers were attached together through Ostwalds ripening depending on the refluxing time and the temperature of the reaction. At higher temperature the capping agent is attached on the surface of the QDs and actively control the agglomeration. Once the temperature of the reaction is reduced, it further reduces the growth of CdTe QDs. Finally the absorption band edges are observed at around 510 nm. The calculated band gap lies between 3 and 2.4 eV depending on the refluxing time. The band gap values are extremely high compared with bulk CdTe, due to the quantum confinement effect of the CdTe QDs.

3.3 Fluorescence Analysis

The fluorescence emission spectra of MSA capped CdTe colloidal QDs for different refluxing time are shown in Fig. 4. All samples show well resolved emission maxima from 480 nm to 580 nm depending on the refluxing time. There is a wavelength difference observed between the

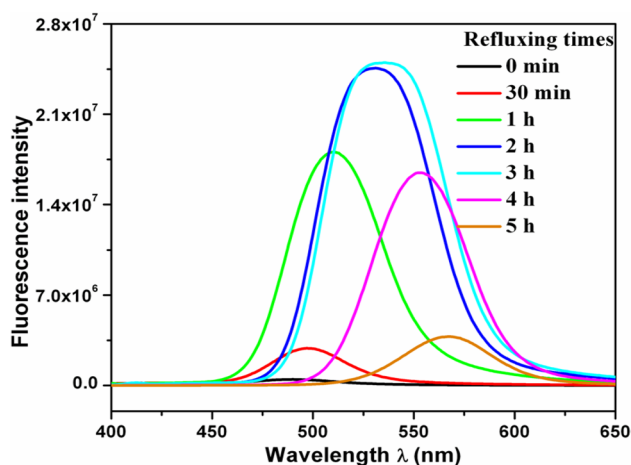


Fig. 4 Fluorescence emission spectra of MSA capped CdTe colloidal QDs for different refluxing times

absorption band edge, and the excitonic emission maximum of the CdTe QDs. This is due to the surface trap state emission of the MSA capped CdTe colloidal QDs. Similar to the absorption band edge, a clear red shift was observed in excitonic emission maximum depending on refluxing time. By increasing refluxing time, the monomer concentration was increased, which results in the aggregation of large number of monomers into highly stable CdTe QDs with larger size. The increase in size of the QDs leads to the red shift in excitonic emission. Along with this red shift, intensity variations in emission peaks are also observed. At longer refluxing time, the monomer concentration is very high. The higher monomer concentration increases the amount of excitonic emission, which leads to the intensity variation with refluxing time. The intensity variations in fluorescence emission peaks clearly indicate that the fluorescence quantum yield was gradually increased with refluxing time. The highest fluorescence emission intensity was observed for 3 h of refluxing time. Similar to that the full width at half maximum values at 3 h was very low compared to other refluxing time. The narrow full width at half maximum values indicates the

Table 2 Band gap values for different refluxing time with their corresponding absorption and emission maximum

Refluxing time (h)	Absorption maximum (nm)	Emission maximum (nm)	Band gap (eV)
0 min	411	489	3.0
30 min	418	497	2.97
1	425	509	2.92
2	432	529	2.87
3	442	538	2.81
4	467	552	2.66
5	502	566	2.47

homogeneous size distribution of QDs. The optical band gap values of MSA capped CdTe QDs for a different refluxing time was calculated from the absorption and emission maximum as listed in Table 2.

3.4 X-ray Diffraction (XRD) Analysis

The crystalline nature of the prepared TiO₂ nanoparticles was studied by powder XRD analysis and the typical XRD patterns of the prepared TiO₂ nanoparticles are shown in Fig. 5. From the XRD patterns, it is revealed that the as-prepared TiO₂ nanoparticles possess the tetragonal crystalline structure with anatase phase. During the post thermal treatment process, the anatase phase of the TiO₂ nanoparticles was converted into rutile phase. The phase transition process of the TiO₂ nanoparticles was clearly identified in the XRD patterns. At 350 °C, TiO₂ nanoparticles possess anatase phase with smaller amount of rutile phase. But, at 700 °C, the quantity of anatase phase was greatly reduced, while the rutile phase was increased. At higher temperatures beyond 900 °C, TiO₂ nanoparticles possess pure rutile phase and the anatase phase completely disappeared. Along with the phase transition, a small size variation was also observed during the post thermal treatment. It means that the size of the TiO₂ nanoparticles was slightly increased with sintering temperature. The average crystallite size of the prepared TiO₂ nanoparticles was estimated by using Scherrer's relation. The average crystallite size of the TiO₂ nanoparticles at 700 °C is 28 nm and the TiO₂ nanoparticles with mixed phases (Anatase & Rutile) was used for the fabrication of QDSSCs.

The powder X-ray diffraction pattern of MSA capped CdTe colloidal QDs synthesized in pH 7 at 95 °C, is shown

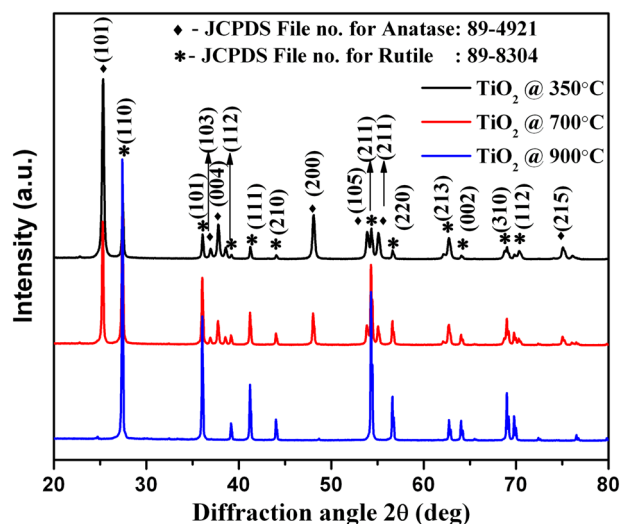


Fig. 5 XRD patterns of TiO₂ nanoparticles

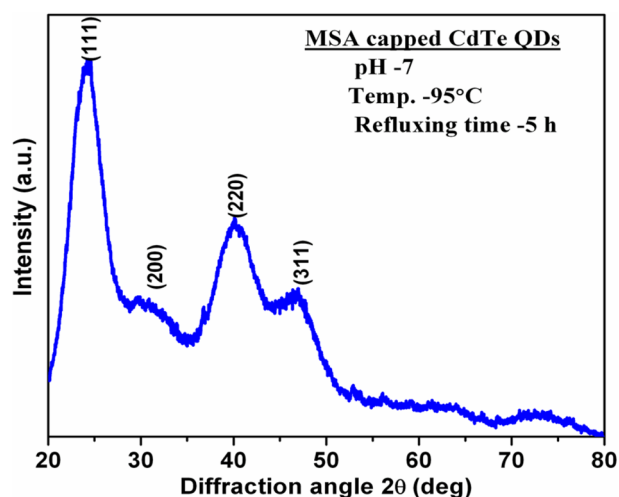


Fig. 6 X-ray diffraction pattern of MSA capped CdTe colloidal QDs

in Fig. 6. The XRD pattern shows the presence of four different diffraction peaks at 2θ values of 24.32, 30.1, 40.2 and 47.3 corresponding to the diffraction planes of (111), (200), (220) and (311) respectively. This is in good agreement with the cubic zinc blende crystalline structure of the bulk CdTe. The average crystallite size of the CdTe colloidal QDs was calculated by using Scherrer's equation.

$$D = 0.9\lambda / \beta \cos \theta \quad (4)$$

where λ is the wavelength of the X-ray source, β is the full width at half maximum of the diffraction peaks and the θ is the diffraction angle. The average crystallite size calculated from XRD is 4 nm.

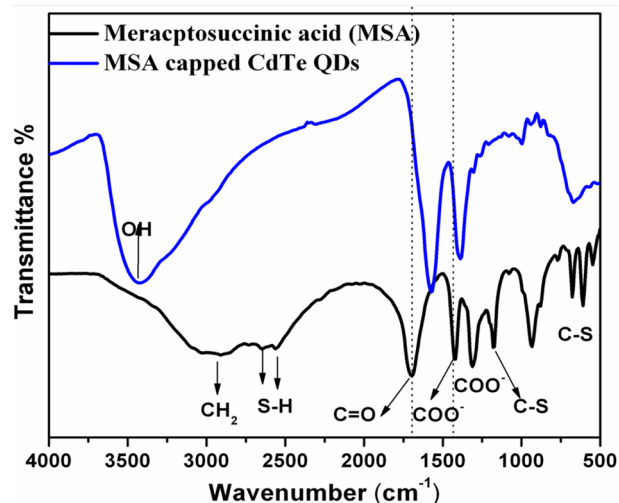


Fig. 7 FT-IR spectra of MSA capped CdTe colloidal QDs

3.5 FT-IR Analysis

The absorption of MSA molecules on the surface of CdTe QDs was studied by the FT-IR analysis. The FT-IR spectra of mercaptosuccinic acid and MSA capped CdTe colloidal QDs are shown in Fig. 7. The broad diffraction peak at around 3400 cm^{-1} is assigned to OH stretching vibrations of water molecules. The active modes of CH_2 vibrations at 2940 cm^{-1} for pure MSA was shifted towards the lower wavenumber for MSA capped CdTe QDs. The lower frequency shift indicates the absorbed surfactant molecules are affected by the solid surface [28]. The S–H vibrations of pure MSA at around 2550 cm^{-1} completely disappeared for MSA capped CdTe colloidal quantum dots. The C=O vibrations at around 1700 cm^{-1} of the MSA was shifted towards lower frequency for MSA capped CdTe QDs. These results indicate that the surface of the CdTe QDs was modified by the MSA molecules through COO^- vibrations instead of COOH in pure MSA. In MSA capped CdTe QDs the symmetric and asymmetric vibrations of COO^- are observed at around 1400 cm^{-1} and around 1300 cm^{-1} , which indicates that MSA molecules are chemisorbed on the surface of Cd^{2+} ions [29]. The presence of various functional groups and their corresponding frequency are listed in Table 3.

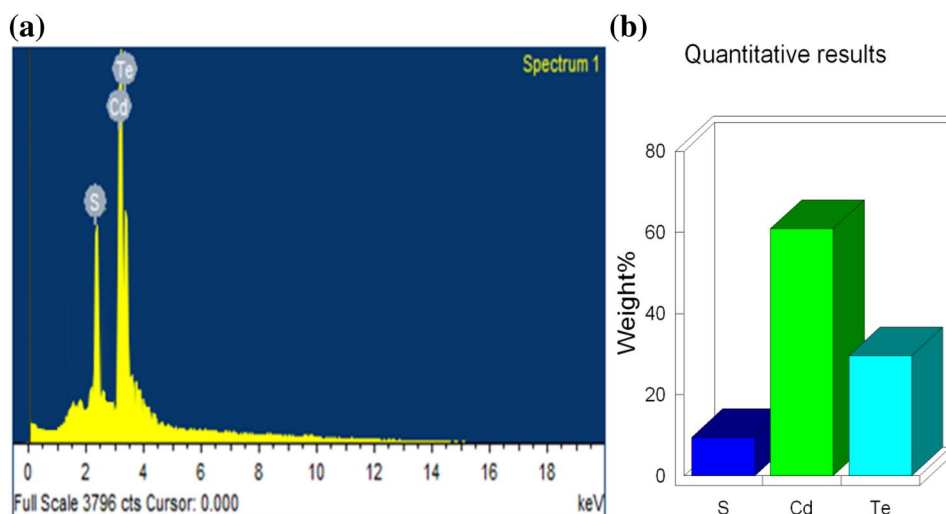
3.6 EDX Analysis

Elemental composition of the prepared QDs was analyzed by the energy dispersive X-ray analysis. Typical EDX spectrum of as prepared MSA capped CdTe QDs are shown in Fig. 8a and the corresponding quantitative analysis in Fig. 8b. Presence of Cd and Te in the EDX spectrum clearly indicates the formation of CdTe QDs with the sulfur functional group of MSA capping

Table 3 Functional groups of pure mercapto succinic acid (MSA) and MSA capped CdTe QDs with their corresponding frequency

Frequency		Functional groups
MSA	MSA capped CdTe	
–	3440	OH stretching vibrations
2931	2916	CH_2 vibrations
2638&2553	–	S–H vibrations
1697	–	C=O vibrations
–	1566	COO^- asymmetric vibrations
1419	–	COOH vibrations
–	1388	COO^- symmetric vibrations
1311	–	C–O stretching vibrations
1180	–	C–O stretch
933	995	C–H bend
678	671	C–S vibrations

Fig. 8 **a** EDX spectrum of MSA capped CdTe QDs, **b** Quantitative result of elemental composition



agent. The quantitative analysis reveals that the prepared CdTe QDs constitute the majority of Cd ions (up-to 60%) and nearly 30% of Te ions. The difference between the amount of Cd and Te ions is probably due to the presence of excessive Cd ions present in the colloidal solution. These excessive Cd ions were reduced during the precipitation process. The formation of defects structure may be another reason for the excessive Cd ions. But there is no defect peaks in XRD and XPS analysis, which reveals that the large amount of Cd ions is derived from the excessive Cd ions present in the as prepared colloidal solution. Smaller portion of sulfur was present due to the capping of MSA molecules.

3.7 XPS Analysis

The XPS spectrum of MSA capped CdTe QDs (Fig. 9) reveals the presence of Cd and tellurium elements with the sulfur functional group of MSA. The presence of carbon and oxygen peaks is also observed in the XPS spectrum due to the absorption of organic carbon from the atmosphere or by the carbon tape used and the absorbed oxygen respectively. The slow scanning spectrum represents the presence of Cd in 3d state with the binding energy of 404.9 eV and Te in 3d state at 571.7 eV. A slight red shift was observed in the binding energy of Cd and Te, compared to pure Cd and Te elements. This is due to the bond formation between the 3d energy states of Cd and Te. The presence of the S functional group due to the absorption of thiol capping agent on the surface of Cd through Cd-SR bonds were observed at 161.9 eV. XPS studies reveal the formation of CdTe QDs with the thiol capping agent on the surface of QDs.

3.8 Thermogravimetric Analysis (TGA)

Thermal stability of MSA capped CdTe QDs was studied by the thermogravimetry analysis (TGA) between 30 and 900 °C at a heating rate of 10°/min as shown in Fig. 10. The TGA spectrum of MSA capped CdTe QDs shows three successive weight losses. The first gradual weight loss observed at around 100 °C is attributed to the removal of water molecules from the surface of CdTe QDs, as confirmed by the OH stretching vibration in FT-IR spectrum. The second evident weight loss in the range 250–350 °C was attributed to the decomposition of chlorides of the precursor material [30]. The third weight loss observed at around 700 °C is due to the decomposition of Cd-MSA complexes. From the TGA analysis, the presence of MSA molecules on the surface of the CdTe QDs upto 700 °C was confirmed.

3.9 Morphological Studies: HR-TEM

Uniform size distribution of MSA capped CdTe QDs was studied by HR-TEM analysis as shown in Fig. 11. Many small spots were observed in HR-TEM image due to the presence of spherical shaped CdTe QDs. The HR-TEM images clearly indicate that the uniform size distribution of 5 nm sized CdTe QDs.

3.10 Fluorescence Images

Fluorescence images of MSA capped CdTe QDs for different refluxing times under visible light and UV irradiations are shown in Fig. 12. Refluxing times 0 min, 15 min, 30 min, 45 min, 1 h, 1.5 h, 2 h, 3 h, 4 h and 5 h are represented by a, b, c, d, e, f, g, h, i and j respectively. In the visible light (Fig. 12A), the prepared QDs

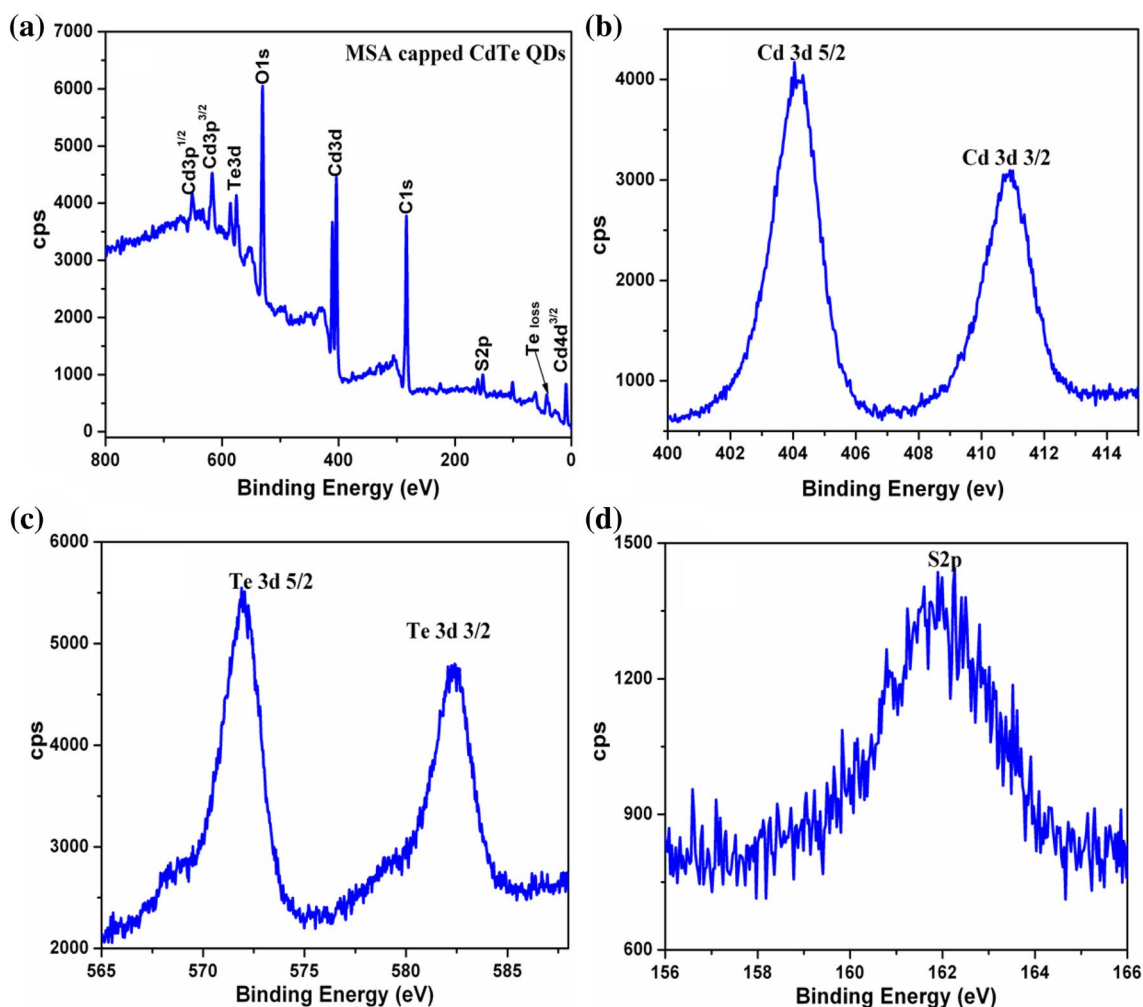


Fig. 9 X-ray photoelectron spectra of MSA capped CdTe QDs. **a** Survey spectrum, **b** Cd, **c** Te and **d** S states

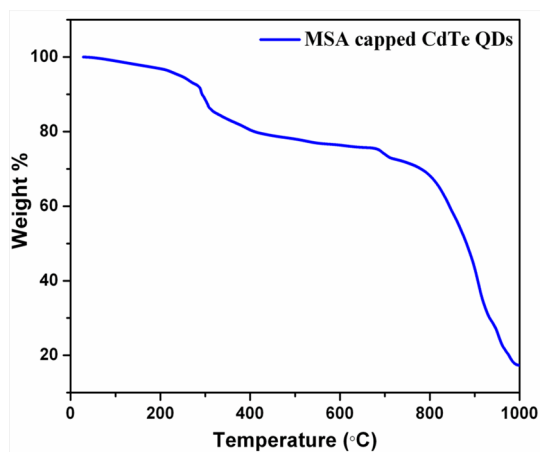


Fig. 10 TGA curve of MSA capped CdTe colloidal QDs

exhibit the fluorescence emission from light green to dark red depending on the increment of refluxing time. At the starting stage of the refluxing time at zero min the QDs show a light green emission. It is due to the smaller size of CdTe QDs. When the duration of the refluxing time was increased to 5 h, the emission color was changed from light green to dark red. This is related to the bigger size of the QDs.

The difference in emission color depending on the refluxing time clearly indicates that the size of the CdTe QDs varies with the refluxing time. At the same time the fluorescence emission color of the CdTe QDs under UV irradiation is different from visible light irradiation (Fig. 12B). The CdTe QDs at zero min of refluxing time show a violet color emission. For smaller QDs the energy of the visible light is not sufficient to overcome the larger energy gap. The emission color variation of MSA capped CdTe QDs is an evidence for the size dependent optical properties of CdTe QDs.

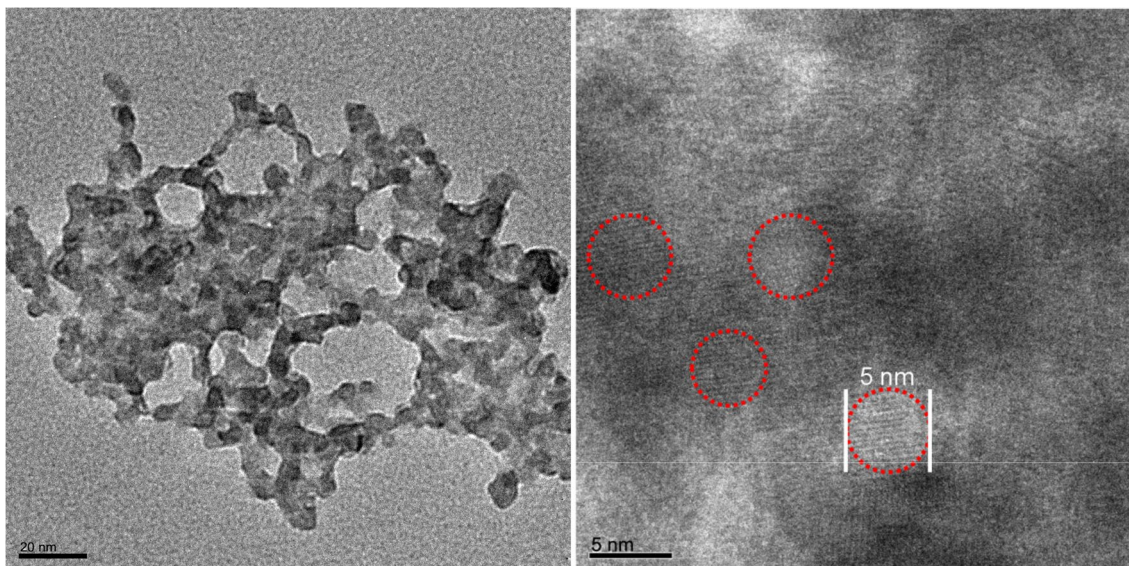
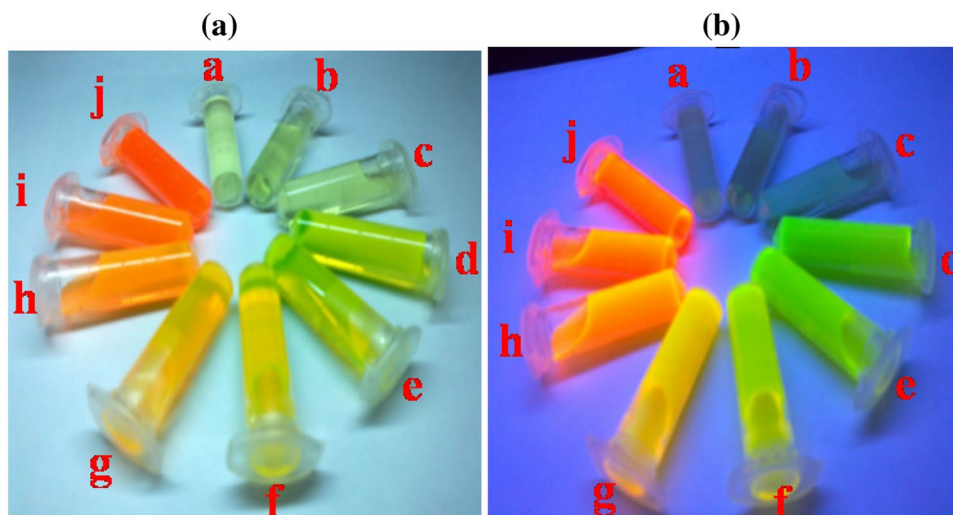


Fig. 11 HR-TEM Images of MSA Capped CdTe Colloidal QDs

Fig. 12 Fluorescence images of MSA capped CdTe colloidal QDs in **A** Visible light and **B** UV light



3.11 Photovoltaic Performance of CdTe QDs Sensitized TiO₂ Photoelectrodes

The photovoltaics performance of the CdTe QDs sensitized TiO₂ photoelectrodes was studied by the J–V characteristic curves under the illumination of sunlight with 1 Sun intensity. The current–voltage characteristic curves of CdTe QDs sensitized solar cells are shown in Fig. 13 and the photovoltaic variables such as open circuit voltage (V_{oc}), short circuit current (J_{sc}), Fill Factor (FF) and the photon conversion efficiency (η) are listed in Table 4.

The photovoltaic variables clearly indicate that the photovoltaics performance of the CdTe QDs sensitized TiO₂ photoelectrodes was increased with sensitization time of the CdTe QDs. The larger sensitization time resulted in

the formation of effective CdTe QDs layer over the TiO₂ nanoparticles. In this process, the CdTe QDs layer acting as a blocking layer to reduce the recombination rate of the electron in the TiO₂ nanoparticles and the hole in the electrolytes, which increases the photovoltaic performances of the photoelectrodes. The short circuit current (J_{sc}) value of CdTe QDs sensitized TiO₂ photoelectrodes were 1.05 mA under the sensitization time of 30 min. Whereas, J_{sc} values were gradually increased with the sensitization time of CdTe QDs. This is due to the effective covering of CdTe QDs over the TiO₂ photoelectrodes. Highest J_{sc} value (2.10 mA) was observed at 3 h of QDs sensitization time. This is due to the increment of photocurrent with the absorption time of CdTe QDs. It clearly indicates that the amount of absorbed CdTe QDs was increased with the sensitization time. The

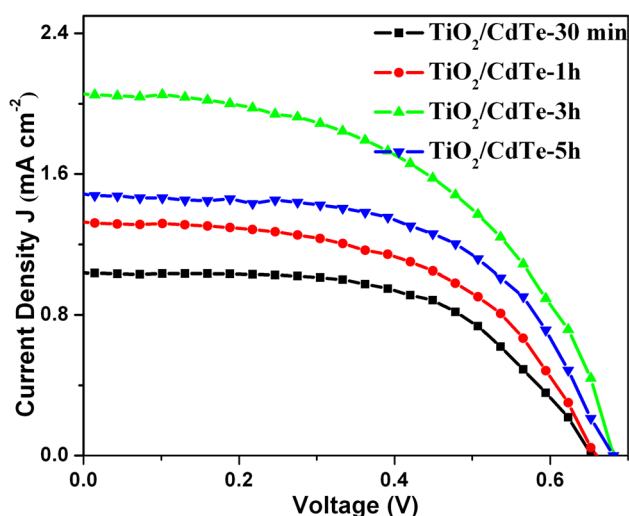


Fig. 13 J–V characteristic curves of CdTe QDs sensitized photoelectrodes for different absorption times

Table 4 Photovoltaic variables of CdTe QDs sensitized photoelectrodes for different absorption time

Sample name	V_{oc} (V)	J_{sc} (mA)	FF	η (%)
TiO ₂ /CdTe-30 min	0.66	1.05	0.56	0.48
TiO ₂ /CdTe-1 h	0.66	1.32	0.54	0.57
TiO ₂ /CdTe-3 h	0.68	2.10	0.50	0.87
TiO ₂ /CdTe-5 h	0.68	1.52	0.54	0.69

maximum photo conversion efficiency of $\eta = 0.87\%$ was observed at 3 h of absorption time. Beyond this absorption time of CdTe QDs, the photovoltaic conversion efficiency was decreased due to the absorption of the large amount of CdTe QDs. Large amount of CdTe QDs increases the recombination rate of electron and hole pairs within the CdTe QDs, resulting in the reduction of charge transport between the electrodes. The overall efficiency of the CdTe QDs sensitized solar cells is still remains very low when compared to CdSe and CdS QDs. This is due to the poor photo stability of the CdTe QDs in polysulfide electrolyte [11].

4 Conclusion

Aqueous phase MSA capped CdTe colloidal QDs for QDSSCs were prepared in ambient atmosphere by using air stable potassium tellurite as a precursor. The effect of precursor concentration on the optical properties of MSA capped CdTe colloidal QDs was systematically studied by varying the molecular ratio between the precursors. Reaction parameters dependent structural and optical properties of MSA capped CdTe QDs were studied under different

reaction conditions. From these studies, pH 7 and 95 °C were selected as the optimal reaction conditions for the preparation of high quality MSA capped CdTe QDs. Similarly, the optimal reaction ratio for the precursors Cd:Te:MSA is 1:0.04:1. Optical studies reveal the size dependent optical properties of MSA capped CdTe QDs under different refluxing time. Cubic zinc blende crystalline structure was confirmed by the XRD analysis. The homogeneous size distribution of CdTe QDs was studied by HR-TEM analysis. Capping of MSA molecules over CdTe QDs was studied by the FT-IR analysis. The elemental composition and the oxidation states of the CdTe QDs formation with the thiol capping agent were revealed by the XPS analysis. The fluorescence images under different refluxing time confirm the size dependent optical properties of CdTe QDs. CdTe QDSSCs were fabricated by using polysulfide electrolytes. J–V measurements reveal that the CdTe QDSSCs show better solar cell efficiency of 0.87% at 3 h of absorption time of CdTe QDs. By the optimization of the fabrication procedures of QDSSC, the solar cell efficiency of CdTe QDSSC may significantly improve.

Acknowledgements This research did not receive any specific grant from funding agencies in the public, commercial, or not-for-profit sectors.

References

- X.G. Peng, L. Manna, W.D. Yang, J. Wickham, E. Scher, A. Kadavanich, A.P. Alivisatos, Shape control of CdSe nanocrystals. *Nature* **404**, 59–61 (2000)
- X.G. Peng, Mechanisms for the shape-control and the shape evolution of colloidal semiconductor nanocrystals. *Adv. Mater.* **15**, 459–463 (2003)
- Z.Y. Tang, Z.L. Zhang, Y. Wang, S.C. Glotzer, N.A. Kotov, Self-assembly of CdTe nanocrystals into free-floating sheets. *Science* **314**, 274–278 (2006)
- M. Achermann, M.A. Petruska, S. Kos, D.L. Smith, D.D. Koleske, V.I. Klimov, Energy transfer pumping of semiconductor nanocrystals using an epitaxial quantum well. *Nature* **429**, 642–646 (2004)
- J. Jiang, K. Wang, Q. Liu, J. Zhai, Optimizing CdS intermediate layer of CdS/CdSe quantum dot-sensitized solar cells to increase light harvesting ability and improve charge separation efficiency. *RSC Adv.* **6**, 99564–99569 (2016)
- Y.-L. Xie, P. Song, S.-Q. Zhao, Preparation of SnS/CdS Co-sensitized TiO₂ photoelectrodes for quantum dots sensitized solar cells. *J. Electron. Mater.* **45**, 4952–4957 (2016)
- C. Yuan, L. Li, J. Huang, Z. Ning, L. Sun, H. Agren, Improving the photocurrent in quantum-dot-sensitized solar cells by employing alloy Pb_xCd_{1-x}S quantum dots as photosensitizers. *Nanomaterials* **6**, 97–113 (2016). <https://doi.org/10.3390/nano6060097>
- F. Shao, M. Li, J. Yang, Y. Liu, L. Zhang, CdSe quantum dot-sensitized solar cell: effect of size and attach mode of quantum dot. *J. Nano Res.* **30**, 78–85 (2015)
- C. Chen, Y. Cheng, J. Jin, Q. Dai, H. Song, CdS/CdSe quantum dots and ZnPc dye co-sensitized solar cells with Au nanoparticles/graphene oxide as efficient modified layer. *J. Colloid Interface Sci.* **480**, 49–56 (2016)

- F. Huang, L. Zhang, Q. Zhang, J. Hou, H. Wang, H. Wang, S. Peng, J. Liu, G. Cao, High efficiency CdS/CdSe quantum dot sensitized solar cells with two ZnSe layers. *ACS Appl. Mater. Interfaces*. **8**(50), 34482–34489 (2016)
- J.H. Bang, P.V. Kamat, Quantum dot sensitized solar Cells. A tale of two semiconductor nanocrystals: CdSe and CdTe. *ACS Nano* **3**, 1467–1476 (2009)
- C.B. Murray, D.J. Norris, M.G. Bawendi, Synthesis and characterization of nearly monodisperse CdE (E = sulfur, selenium, tellurium) semiconductor nanocrystallites. *J. Amer. Chem. Soc.* **115**, 8706–8715 (1993)
- D.V. Talapin, S. Haubold, A.L. Rogach, A. Kornowski, M. Haase, H. Weller, A novel organometallic synthesis of highly luminescent CdTe nanocrystals. *J. Phys. Chem. B* **105**, 2260–2263 (2001)
- Y.W. Cao, U. Banin, Growth and properties of semiconductor core/shell nanocrystals with InAs cores. *J. Amer. Chem. Soc.* **22**, 9692–9702 (2000)
- L. Spanhel, M. Haase, H. Weller, A. Henglein, Photochemistry of colloidal semiconductors. 20. Surface modification and stability of strong luminescing CdS particles. *J. Amer. Chem. Soc.* **109**, 5649–5655 (1987)
- M.T. Harrison, S.V. Kershaw, M.G. Burt, A. Eychmuller, H. Weller, A.L. Rogach, Wet chemical synthesis and spectroscopic study of CdHgTe nanocrystals with strong near infrared luminescence. *Mater. Sci. Eng. B*. **69**, 355–360 (2000)
- S. Reghuram, A. Arivarasan, R. Kalpana, R. Jayavel, CdSe and CdSe/ZnS quantum dots for the detection of C-reactive protein., *J. Exp. Nanosci.* **2014**, 902542-16 (2014)
- A. Wang, L. Fu, T. Rao, W. Cai, M.-F. Yuen, J. Zhong, Effect of Metal ions on the quenching of photoluminescent CdTe QDs and their recovery. *Opt. Mater.* **46**, 350–354 (2015)
- C.D. Gutiérrez-Lazos, M. Ortega-López, E. Rosendo-Andrés, Y. Matsumoto-Kuwabara, V. Sánchez-Reséndiz, J. Morales-Corona, R. Olayo-González, E. Barrera-Calva, T. Díaz-Becerril, Highly luminescent CdTe nanocrystals synthesized in aqueous solution and self-assembled on polyelectrolyte multilayers. *Mater. Sci. Forum.* **374**, 636–637 (2010)
- H. Zhang, Z. Zhou, B. Yang, M.Y. Gao, The influence of carboxyl groups on the photoluminescence of mercaptocarboxylic acid-stabilized CdTe nanoparticles. *J. Phys. Chem. B* **107**, 8–13 (2003)
- A. Ayyaswamy, S. Ganapathy, A. Alsalmeh, A. Alghamdi, J. Ramasamy, Structural, optical and photovoltaic properties of codoped CdTe QDs for quantum dots sensitized solar cells. *Superlattice Microst.* **88**, 634–644 (2015)
- M.S. Abd El-sadek, J.R. Kumar, S.M. Babu, The role of potassium tellurite as tellurium source in mercaptoacetic acid-capped CdTe nanoparticles. *Cur. Appl. Phys.* **10**, 317–322 (2010)
- A. Badawi, N. Al-Hosiny, S. Abdallah, S. Nagm, H. Talaat, CdTe quantum dots sensitized TiO₂ electrodes for photovoltaic cells. *J. Mater. Sci. Eng. A* **1**, 942–947 (2011)
- G. Syrokostas, M. Giannoulis, P. Yianoulis, Effects of paste storage on the properties of nanostructured thin films for the development of dye-sensitized solar cells. *Renew. Energy* **34**, 1759–1764 (2009)
- L. Li, H. Qian, N. Fang, J. Ren, Significant enhancement of the quantum yield of CdTe nanocrystals synthesized in aqueous phase by controlling the pH and concentrations of precursor solutions. *J. Lumin.* **116**, 59–66 (2006)
- H. Zhang, L.P. Wang, H.M. Xiong, L.H. Hu, B. Yang, W. Li, Hydrothermal synthesis for high quality CdTe QDs. *Adv. Mater.* **15**, 1712–1715 (2003)
- L. Li, L.H.F. Qian, J.C. Ren, Rapid synthesis of highly luminescent CdTe QDs in the aqueous phase by microwave irradiation with controllable temperature. *Chem. Commun.* **36**, 528–530 (2005)
- M.S. Abd El-sadek, S.M. Babu, A controlled approach for synthesizing CdTe@CrOOH (core-shell) composite nanoparticles. *Cur. Appl. Phys.* **11**, 926–932 (2011)
- K.V. Mrudula, T.U.B. Rao, T. Pradeep, Interfacial synthesis of luminescent 7 kDa silver clusters. *J. Mater. Chem.* **19**, 4335–4342 (2009)
- T. Erdmenger, J. Vitz, F. Wiesbrock, U.S. Schubert, Influence of different branched alkyl side chains on the properties of imidazolium-based ionic liquids. *J. Mater. Chem.* **18**, 5267–5273 (2008)